A Transgenic Animal Model of Osmotic Cataract. Part 1: Over-expression of Bovine Na^+/Myo-inositol Cotransporter in Lens Fibers

Patrick R. Cammarata,[1] Cheng Zhou,[1] Guoli Chen,[1] Inderpal Singh,[1] Rustin E. Reeves,[1] Jerome R. Kuszak,[2] and Michael L. Robinson[3]

Purpose. Intracellular osmotic stress is believed to be linked to the advancement of diabetic cataract. Although the accumulation of organic osmolytes (myo-inositol, sorbitol, taurine) is thought to protect the lens by maintaining osmotic homeostasis, the physiologic implication of osmotic imbalance (i.e., hyperosmotic stress caused by intracellular over-accumulation of organic osmolytes) on diabetic cataract formation is not clearly understood. Studies from this laboratory have identified several osmotic compensatory mechanisms thought to afford the lens epithelium, but not the lens fibers, protection from water stress during intervals of osmotic crisis. This model is founded on the supposition that the fibers of the lens are comparatively more susceptible to damage by osmotic insult than is the lens epithelium. To test this premise, several transgenic mouse lines were developed that over-express the bovine sodium/myo-inositol cotransporter (bSMIT) gene in lens fiber cells.

Methods. Of the several transgenic mouse lines generated, two, MLR14 and MLR21, were analyzed in detail. Transgenic mRNA expression was analyzed in adult and embryonic transgenic mice by a coupled reverse transcriptase–polymerase chain reaction (RT–PCR) and in situ hybridization on embryonic tissue sections, respectively. Intralenticular myo-inositol content from individual mouse lenses was quantified by anion exchange chromatography and pulsed electrochemical detection. Ocular histology of embryonic day 15.5 (E15.5) embryos from both transgenic (TG) families was analyzed and compared to their respective nontransgenic (NTG) littermates.

Results. Both RT–PCR and in situ hybridization determined that transgene expression was higher in line MLR21 than in line MLR14. Consistent with this, intralenticular myo-inositol from MLR21 TG mice was markedly higher compared with NTG littermates or MLR14 TG mice. Histologic analysis of E15.5 MLR21 TG embryos disclosed a marked swelling in the differentiating fibers of the bow region and subcapsular fibers of the central zone, whereas the lens epithelium appeared morphologically normal. The lenticular changes, initiated early during lens development in TG MLR21 embryos, result in severe bilateral nuclear cataracts readily observable in neonates under normal rearing and dietary conditions. In contrast, TG MLR14 pups reared under standard conditions produced no lens opacity.

Conclusions. Lens fiber swelling and related cataractous outgrowth positively correlated to the degree of lens bSMIT gene expression and intralenticular myo-inositol content. The affected (i.e., swollen) lens fibers appeared to be unable to cope with the water stress generated by the transgene-induced over-accumulation of myo-inositol and, as a result of this inability to osmoregulate, suffered osmotic damage due to water influx. (*Invest Ophthalmol Vis Sci.* 1999;40:1727–1737)

The lens must be able to endure periods of variation in lenticular osmolarity, such as might be encountered with glucose-derived osmotic stress in the diabetic condition. The lens compensates for water stress by accumulating osmotically active nonperturbing organic solutes or osmolytes.[1] Three putative organic osmolytes have been identified in cultured lens epithelial cells, namely, sorbitol,[2] myo-inositol,[3,4] and taurine.[5] Studies from this laboratory have primarily focused on myo-inositol utilization and have previously shown that cultured bovine lens epithelial cells (BLECs) respond to hyperosmotic insult with increased transcription of Na^+/myo-inositol cotransporter mRNA, resulting in increased Na^+/myo-inositol cotransporter protein synthesis and osmolyte (i.e., myo-inositol) accumulation. To modulate their intracellular store of myo-inositol, BLECs, utilize three osmotic compensatory mechanisms: suppression or activation of myo-inositol cotransporter activity,[6] regulation of Na^+/myo-inositol cotransporter gene transcription,[7] and attenuation or stimulation of myo-inositol passive permeability from cell to extracellular medium via a chloride-associated, myo-inositol efflux channel.[8] The intracellular accumulation of myo-inositol and other compatible organic osmolytes operates to maintain os-

From the [1]Department of Anatomy and Cell Biology, University of North Texas Health Science Center at Fort Worth/North Texas Eye Research Institute, Fort Worth, Texas; the [2]Departments of Pathology and Ophthalmology, Rush–Presbyterian–St. Luke's Medical Center, Chicago, Illinois; and the [3]Department of Pediatrics, The Ohio State University and Children's Hospital Research Foundation, Columbus, Ohio.

Supported by National Health Public Service Award EY05570–12 (PRC) and Children's Hospital Research Foundation (MLR).

Presented at the annual meeting of the Association for Research in Vision and Ophthalmology, Fort Lauderdale, Florida, May 1999.

Submitted for publication January 27, 1999; revised March 17, 1999; accepted March 23, 1999.

Proprietary interest category: N.

Reprint requests: Patrick R. Cammarata, Department of Anatomy and Cell Biology, University of North Texas Health Science Center/North Texas Eye Research Institute, 3500 Camp Bowie Boulevard, Fort Worth, TX 76107.

motic homeostasis and to protect the cell against the perturbing effects of high intracellular concentrations of electrolytes that might otherwise adversely affect protein structure and function.

The "osmotic compensation" phenomenon of myo-inositol uptake and efflux likewise functions in the bovine lens via the lenticular anterior epithelium.[9] In the course of evaluating recent organ culture studies, we became aware that [^{3}H]–myo-inositol, although readily taken up, fluxed across the lenticular anterior epithelial plasma membrane, or both, did not readily cross the plasma membrane of the lens fibers.[9] That and additional observations prompted us to speculate that a function of the lenticular epithelium was to protect itself during periods of extracellular osmotic fluctuation or chronic aberrant intracellular polyol accumulation. The lenticular epithelium can mobilize one or more of the osmotic compensatory mechanisms discussed above. Implicit in that formulation, however, was also the principle that "during the course of safeguarding itself, the epithelium, may, inadvertently influence . . . the intracellular osmotic homeostasis of the (subjacent) fiber cells, which likely have diminished capability to osmoregulate."[9]

The studies described herein were based on the premise that the fiber cells of the lens, unlike the lens epithelium, are characterized by an increased susceptibility to osmotic damage, in large part because of an inability to adequately osmoregulate. To authenticate this idea, several mouse lines were developed that over-express the bovine Na^+/myo-inositol cotransporter (bSMIT) gene in lens fibers with resulting overaccumulation of myo-inositol. A positive correlation between the degree of lens bSMIT gene expression and the proportion of intralenticular myo-inositol content relative to the progression of nuclear cataractous development is shown.

Materials and Methods

Isolation of bSMIT Genomic DNA

A bovine liver genomic library in EMBL-3 SP6/T7 vector (Clontech, Palo Alto, CA) was screened. Approximately 2×10^6 bacteriophage plaques were screened with the [^{32}P]-labeled 626-bp cDNA probe, which is located near the 3′-end of the open reading frame (ORF) of the bovine Na^+/myo-inositol cotransporter gene.[10] Positive phage clones were digested with *Xho*I and further characterized by Southern hybridization using the 626-bp cDNA probe. An approximate 15-kb genomic fragment was isolated and subcloned into pBluescript (Stratagene, La Jolla, CA) and designated bSMIT2. bSMIT2 was digested with *Kpn*I and subsequent Southern blot analysis identified an 8.2-kb fragment that contained the entire bSMIT ORF. This fragment was subsequently subcloned into pBluescript vector and designated bSMIT2K8.2.

Construction of CPV14/bSMIT

The entire SMIT ORF was polymerase chain reaction (PCR)–amplified from the genomic clone bSMIT2K8.2 using the sense primer, 5′-*CGGAATTC*TTACCAAAC***ATG***AGGGCTGT-3′ and the antisense primer, 5′-*CGGAATTC*CTCATCATATCCTTAAAAGT-3′. The sense primer encompassed the initiation codon (indicated by bold sequence) for the bSMIT ORF. The antisense primer encompassed sequences after the termination codon (2176–2156 relative to the ATG). Artificial *Eco*RI linker sequences (italicized) were added to the 5′ end of each primer to facilitate cloning. Because there are no introns within the coding sequence of bSMIT,[11] the PCR-amplified clone from genomic DNA represents the same size and sequence as the representative bSMIT mRNA. The resultant PCR-produced bSMIT cDNA clone was subcloned into the *Eco*RI site of the crystallin promoter vector CPV14 and was subsequently completely sequenced to ensure the absence of any PCR-generated mutations. CPV14 is an αA-crystallin promoter vector identical to CPV2[12] with the exception of an insertion of 30 bp of artificial sequence at −83 relative to the endogenous transcription start site of the murine αA-crystallin gene. This 30-bp sequence, ATCC***ATCTTCACGCATGAGTGACT***GGATCT contains a consensus binding site (boldfaced) for the Pax-6 transcription factor[13] that was added to enhance the expression of transgenes driven by the −282/+43 murine αA-crystallin promoter.[14] Like CPV2, CPV14 contains the small t intron and polyadenylation sequences from the SV40 virus early region[15] downstream of the *Eco*RI site into which the bSMIT cDNA was cloned. The 3515-bp transgene construct was released from vector sequences by digestion with *Not*I and subsequently was purified by agarose gel isolation using Qiaex II (Qiagen, Valencia, CA).

Transgenic Mice

The isolated microinjection construct was eluted in 10 mM Tris–HCl (pH 7.4) 0.1 mM EDTA and injected into pronuclear stage FVB/N embryos at a concentration of 2 ng/μl. Injected embryos were transferred into pseudopregnant ICR strain female mice. Potential transgenic offspring were screened for by isolating genomic DNA from tail biopsies and testing for transgenic sequences by PCR. The following primers were used for PCR analysis: (C4) 5′-GCATTCCAGCTGCTGACGGT-3′, a sense primer to the murine αA-crystallin promoter; (B1) 5′-CGCCCCGCCAAGAAGTATCCA-3′, an antisense primer to the bSMIT coding region; (S5) 5′-GTGAAGGAACCTTACTTCTGTGGNTG3′, a sense primer to the SV40 virus early region upstream of the intron splice site; and (S3) 5′-GTCCTTGGGGTCTTCTACCTTTCTC-3′, an antisense primer to the SV40 virus early region downstream from the intron splice site. Primers C4 and B1 amplify a 380-bp fragment from the 5′-region of the transgene, and primers S5 and S3 amplify a 300-bp fragment from the 3′-region of the transgene using transgenic genomic DNA as a PCR template.

In Situ Hybridization

An *Eco*RI/*Xba*I fragment of CPV2 containing the entire 877-bp SV40 intron and polyadenylation sequence was subcloned into Bluescript KS$^-$ (Stratagene) to generate a riboprobe vector as previously described.[12] Sense and antisense transcripts were produced by in vitro transcription using 1 μg linearized riboprobe vector with 20 U of T3 (Stratagene) and 20 U of T7 (Pharmacia, Piscataway, NJ) RNA polymerase, respectively, for 3 hours at 30°C using ^{35}S-labeled UTP as previously described.[11] Hybridizations were performed on embryos collected from timed pregnancies (morning of copulation plug = day E0.5). The embryos were fixed in 4% paraformaldehyde, dehydrated, and embedded in PARAPLAST X-TRA embedding wax (Oxford Labware, St. Louis, MO). Tissue sections (5 μm) were collected on Superfrost Plus microscope slides (Fisher Scientific, Fair Lawn, NJ), deparaffinized in xylenes, and rehydrated in a decreasing ethanol series. Sections were treated

with 0.2 N HCl for 15 minutes, rinsed in phosphate-buffered saline and incubated in 20 μg/ml proteinase K (GIBCO/BRL, Rockville, MD) in 50 mM Tris, pH 7.5; 5 mM EDTA for 7 minutes at 25°C. Slides were rinsed in 4% glycine/phosphate-buffered saline and acetylated with 0.25% acetic anhydride made in 0.2 M triethanolamine–HCl, pH 8.0. Hybridizations were carried out overnight at 50°C in 0.3 M NaCl/10 mM Tris–HCl, pH 7.4/10 mM NaH_2PO_4/5 mM EDTA/0.2% Ficoll 400/0.2% polyvinyl pyrrolidone/50 mM dithiothreitol/0.5 mg/ml polyadenylic acid/50 mg/ml yeast tRNA/10% dextran sulfate/50% formamide/0.25 mM γ-S-thio ATP (Sigma Chemical, St. Louis, MO). Approximately 20 ng of ^{35}S-labeled sense or antisense riboprobe/slide was added to the hybridization mixture. Slides were washed in: FSM (50% formamide/0.3 M NaCl/30 mM citric acid, pH 8.0/20 mM β-mercaptoethanol) at 65°C twice for 30 minutes; STE (0.6 M NaCl/60 mM citric acid, pH 8.0/20 mM Tris–HCl, pH 7.4/1 mM EDTA) at 37°C twice for 10 minutes; STE supplemented with 6 μg/ml RNase A at 37°C for 30 minutes; STE supplemented with 20 mM β-mercaptoethanol at 37°C for 10 minutes; FSM at 65°C twice for 45 minutes; 0.3 M NaCl/30 mM citric acid, pH 8.0 at 37°C for 10 minutes; and 15 mM NaCl/1.5 mM citric acid, pH 8.0 at 25°C for 5 minutes. Hybridized slides were air-dried, dipped in Kodak NTB-2 emulsion, and exposed for 4 days at 4°C before being developed with Kodak D-19 developer. Slides were counterstained with hematoxylin and eosin.

Reverse Transcriptase–Polymerase Chain Reaction

Mouse lenses were removed aseptically, and each lens was transferred to a preweighed 1.5-ml microfuge tube. The weight of each lens was determined before extraction of total RNA. Four hundred microliters of RNAZol (Cinna/Biotecx Laboratories, Houston, TX) was added to each tube containing a single mouse lens. Each lens was homogenized using several strokes with a microfuge tube pestle with subsequent addition of 40 μl chloroform. The samples were vigorously mixed for 15 seconds, kept on ice for 5 minutes, and subsequently centrifuged at 12,000*g* (4°C) for 15 minutes. After centrifugation, the upper aqueous phase was transferred to a fresh tube, an equal volume of isopropanol was added to each sample, and the samples were stored overnight at −20°C. Samples were subsequently centrifuged at 12,000*g* (4°C) for 15 minutes, the supernatant removed, and the RNA pellet washed once with 400 μl 75% ethanol by vortexing with subsequent centrifugation for 8 minutes at 7500*g* (4°C). The pellet was dried in vacuo for 15 minutes, and the dried pellet dissolved in 20 μl of deionized water at 65°C for 15 minutes and the absorbance of RNA measured at A260 and A280.

Reverse transcription was performed on 2.5 μg of total RNA in a 20-μl total volume containing oligo$(dT)_{16}$, 5 mM $MgCl_2$, 1× buffer II (Perkin Elmer, Branchburg, NJ), 50 U MuLVRT, and 20 U RNase inhibitor. For PCR, 2 μl of the above cDNA was amplified in 50 μl of total volume containing 1× buffer II, 2.5 mM each of 5′ primer and 3′ primer, 0.75 mM $MgCl_2$, 0.2 mM each of dNTPs, 1.25 U of *Taq* polymerase, and 2 μCi ^{32}P-dCTP (3000 Ci/mmol). Oligonucleotides used to detect transgenic transcripts were S5 and S3 (described above), sense and antisense primers flanking the small t intron from SV40 virus present at the 3′ end of the transgenic construct. Although S5 and S3 amplify a 300-bp band from transgenic genomic DNA, a 236-bp band is amplified by properly spliced transgene transcripts reverse-transcribed into cDNA. β-Actin transcripts were amplified using the sense oligonucleotide 5′-AGGCCAACCGCGAGAAGATGACC-3′ and the antisense oligonucleotide 5′-GAAGTCCAGGGCGACGTAGCAC-3′ (Integrated DNA Technologies, Coralville, IA). Separate PCR tubes were used to amplify transgene transcripts and β-actin transcripts. The PCR was performed using an initial denaturation for 3 minutes at 94°C followed by 30 to 32 cycles of denaturation at 94°C for 30 seconds, annealing at 57°C to 60°C for 30 seconds, and extending at 72°C for 30 seconds in a GeneAmp PCR System 9700 (PE Applied Biosystems, Norwalk, CT). The final cycle, of 30 to 32 cycles, was followed by a 5-minute extension period at 72°C. The cDNA products were separated on a 6% polyacrylamide 7 M urea denaturing gel at 2000 V for 2 hours. The bands were visualized by exposure to x-ray film for 20 hours at −70°C.

Determination of Intralenticular Myo-Inositol

Intralenticular myo-inositol content from individual mouse lenses was quantified by anion exchange chromatography and pulsed electrochemical detection using a Dionex BioLC chromatography system (Dionex, Sunnyvale, CA). Mouse lenses were removed from freshly excised eyes under aseptic conditions, immediately weighed, and stored at −80°C in a 1.5-ml microcentrifuge tube until further analysis. For myo-inositol determination, each lens was individually placed into a 2-ml Dounce homogenizer with addition of 350 μl of 0.3 N zinc sulfate (Sigma Chemical), the lens ground, and the suspension transferred into a 30-ml glass Corex ultracentrifuge tube. Further cell disruption was accomplished by rapid freezing in liquid nitrogen followed by rapid thawing at 37°C for a total of three repetitions. Thereafter, the samples were transferred back to a 5-ml Dounce homogenizer and subjected to an additional five strokes, all the while being maintained in an ice bath. The homogenate was then placed into a Corex ultracentrifuge tube, the homogenizer subsequently rinsed with 150 μl of 0.3 N zinc sulfate, and the rinse combined with the initial suspension. The combined homogenate was centrifuged at 18,000*g* at 4°C for 20 minutes. The resulting supernatant was removed and adjusted to 0.5 ml with 0.3 N zinc sulfate with the further addition of 0.5 ml of 0.3 N barium hydroxide (Sigma Chemical). This suspension was centrifuged at 2500*g* at 4°C for 10 minutes, and the supernatant was subsequently removed and stored without further modification at −20°C for later myo-inositol determination.

Statistical Analysis

Intralenticular myo-inositol determinations are expressed as mean ± SEM. Data were analyzed by ANOVA followed by Tukey HSD multiple group comparisons using Systat 5.2 (Systat, Evanston, Il).

Animal Care

All procedures concerning animals in this study adhered to the ARVO Statement for the Care and Use of Animals in Ophthalmic and Vision Research. All mice were permitted ad libitum food and water and maintained on a 12-hour dark–12-hour light cycle (lights on at 6 AM). The mice were maintained on a standard rodent diet (Harlan–Teklad, Madison, WI) of 19% protein, 5% fat, and 5% crude fiber.

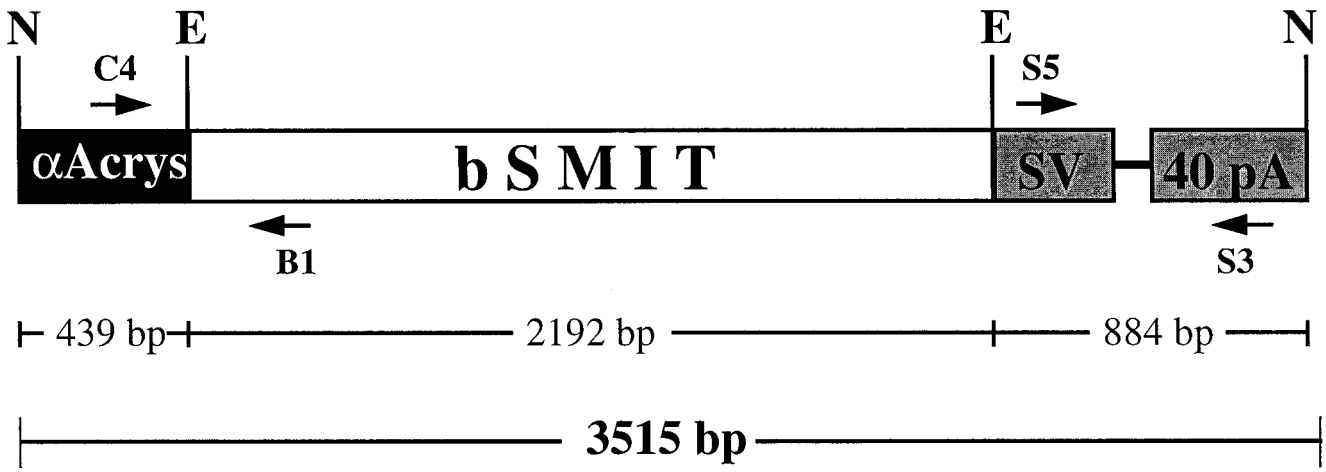

FIGURE 1. The CPV14/bSMIT transgenic construct. The coding sequences for the bovine Na^+/myo-inositol cotransporter (bSMIT) were cloned into the *Eco*RI(E) site of the modified αA-crystallin promoter vector CPV14 (see Materials and Methods). The promoter is indicated by the *black box*, the coding sequences by the *open box*, and the 3′ SV40 virus derived intron and polyadenylation sequences are indicated by the *interrupted gray box*. The entire microinjection construct was released from vector sequences by digestion with *Not*I(N) to yield the 3515-bp transgenic microinjection construct depicted. The locations of primers C4, B1, S5, and S3 (described in Materials and Methods) used for PCR analysis of transgenic mice are indicated.

RESULTS

We developed a transgenic construct to over-express the Na^+/myo-inositol cotransporter in the lens fiber cells of transgenic mice to test whether these mice would become susceptible to the formation of osmotic cataract. The cloned bovine Na^+/myo-inositol cotransporter cDNA,[7] which encodes a myo-inositol transport protein, was fused to a modified version of the murine αA-crystallin promoter, used because of its specificity of lens gene expression (Fig. 1). The hybrid gene CPV14/bSMIT was injected into pronuclear stage FVB/N embryos, transferred into pseudopregnant female mice, and allowed to go to term under normal rearing conditions. Six transgenic founder mice displaying one of two phenotypes were produced. Two of these founders developed bilateral nuclear cataracts, and this phenotype was transmitted to transgenic offspring in subsequent generations in both families. The other four transgenic founders did not exhibit cataracts under standard dietary conditions. Two transgenic lines, one displaying spontaneous cataracts (MLR21) and one characterized by clear lenses (MLR14), have been characterized to date and are the subject of all further discussion in this manuscript.

Nuclear Cataract in the Transgenic Mouse Lens

Figure 2A shows the eye of a 9-week-old transgenic mouse from the family MLR21. Note the presence of a dense nuclear cataract. The lens of the nontransgenic age-matched littermate is clear (Fig. 2B), as are the lenses of 9-week-old transgenic (Fig. 2C) and nontransgenic (Fig. 2D) mice from the family MLR14. Figure 3 shows our initial structural examination comparing a thick polar axis section of a 7-week-old (Fig. 3A) transgenic ($n = 5$) mouse from the family MLR21 versus its (Fig. 3B) nontransgenic ($n = 6$) age-matched littermate. The lens epithelium of both the transgenic and nontransgenic mice was normal. Fiber formation in the bow region of these adult mice was also relatively unaffected in both groups, except that the bow region appeared "pushed up" with the transgenic mice. However, the mature secondary fibers of 7-week-old transgenic mice showed abnormalities along their length. Their equatorial segments were vacuolated, whereas their anterior and posterior segments were protracted, swollen, lacked typical opposite end curvature, and clearly failed to overlap and form normal suture branches between and within successive growth shells. Additional work in progress will be necessary to establish whether these secondary fiber abnormalities are initiated before or after fiber maturation.

Specificity and Localization of Transgenic mRNA

The transgene promoter used in these studies was identical to the −282/+43 murine αA-crystallin promoter commonly used to direct transgene expression to the lens[12] with the addition of a 30-bp Pax-6 consensus binding site[13] designed to enhance transgene expression in the lens. The tissue specificity of the promoter was assayed by a coupled RT–PCR from total RNA extracted from an assortment of tissues taken from a 10-week old transgenic mouse from the family MLR21 (Fig. 4). CPV14/bSMIT expression predominates in transgenic lenses, with very low expression in spleen and lung likewise being noted. Trace transgene expression was also observed in the brain, kidney, and heart; no expression was apparent in muscle or liver.

A coupled RT–PCR was performed from total RNA extracted from 10-week-old individual lenses, from nontransgenic and transgenic littermates, from both families, to determine whether the variation in phenotype between the two transgenic families, MLR21 and MLR14, correlated with differences in the level of transgene mRNA (Fig. 5). The relative level of transgene transcript expression from individual transgenic lenses may be approximated from the densities of transgene-specific PCR product (amplified using primers S5 and S3) and β-actin PCR product as shown in Figure 5. As expected, the 236-bp band, specific for the properly spliced transgene transcripts, was only detected in transgenic lenses from both transgenic families as demonstrated by the exclusive presence of the β-actin–specific band in nontransgenic samples. Note the relative uniformity of gene expression from one transgenic lens to the next within the age-matched litter in both the top

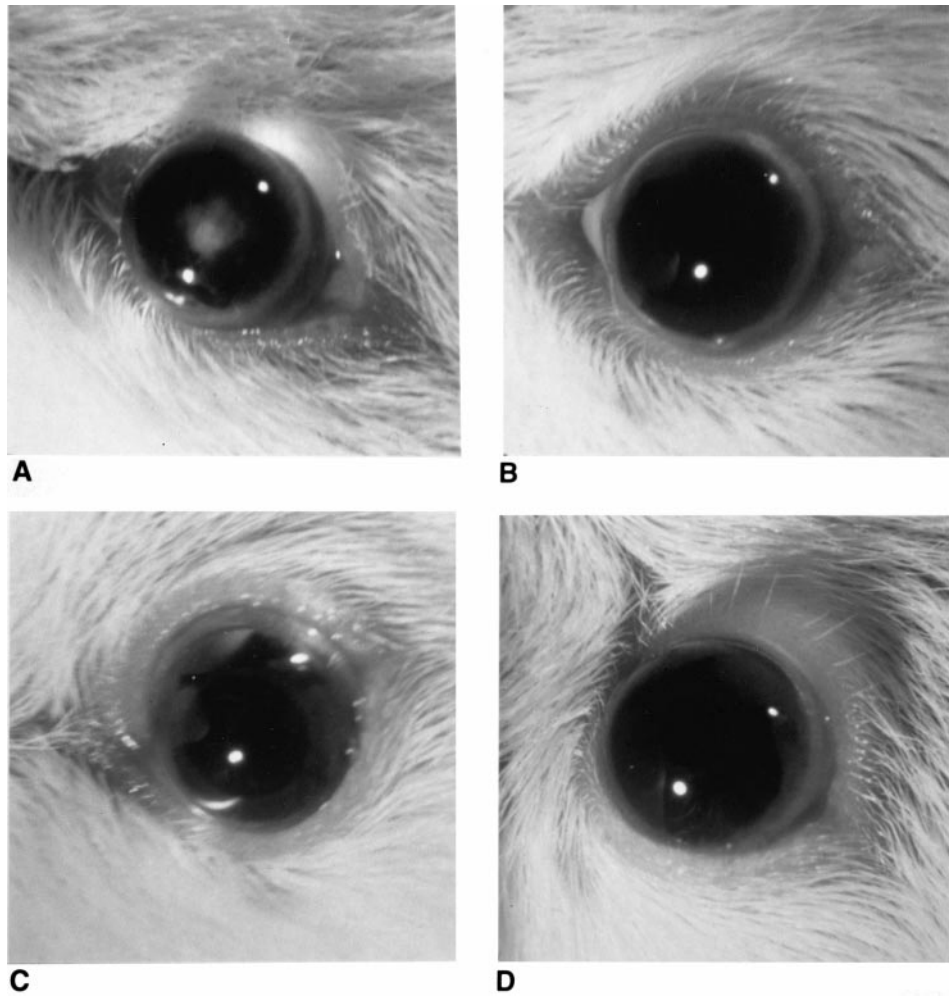

FIGURE 2. Cataract development in transgenic mice. (**A**) Eye of a 9-week-old transgenic mouse from the family MLR21, showing a dense nuclear cataract. (**B**) Eye of a nontransgenic littermate showing no cataract. Eye of a 9-week-old transgenic mouse (**C**) and nontransgenic littermate (**D**) from the family MLR 14, showing no sign of cataract.

(MLR21 litter) and bottom (MLR14 litter) panels of Figure 5. Notice, however, that in both top and bottom panels the intensity of the transgene-specific band is similar. This contrasts with the intensity of the β-actin signal, which is much more intense in the samples from the lower panel (from MLR14). Thus, a visual comparison of transgene PCR product to β-actin PCR product between the two different families reveals considerably lower transgene expression among the transgenic mice of MLR14 relative to the transgenic mice of MLR21.

Although we fully expected the CPV14bSMIT to express in the lens fiber cells, we were aware that the inclusion of the 30-bp Pax-6 consensus element might drive transgene expression in the lens epithelium as well.[14] In situ hybridization was used to localize transgenic transcripts within the developing lens and to determine whether there was any detectable nonlens expression of the transgene in other tissues that express Pax-6, such as other parts of the eye and brain. The entire SV40 portion of the transgenic construct was used to generate an antisense riboprobe that would specifically detect transgenic transcripts by in situ hybridization. This analysis, performed on transverse sections of embryonic heads at embryonic day 15.5 (E15.5), detected transgenic transcripts exclusively in the lens fiber cells of transgenic embryos from both families (Fig. 6). No hybridization signals were detected in the lens epithelium from either transgenic family, consistent with the expression pattern typically seen by transgenes driven by the −366/+46 murine αA-crystallin promoter[16] or the 282/+43 murine αA-crystallin promoter of CPV2.[12] Strong transgene-specific hybridization signals confirmed that the CPV14/bSMIT transgene was expressed at high levels in the developing lens of transgenic MLR21 embryos (Figs. 6A, 6B), whereas much weaker hybridization signals detected in the developing lens of MLR14 (Figs. 6E, 6F) indicated a low level of transgene expression in this family. No specific hybridization was detected with the sense riboprobe on MLR21 transgenic lenses (Figs. 6C, 6D) or the antisense transgene-specific riboprobe on nontransgenic lens sections (Figs. 6G, 6H).

Determination of Intralenticular Myo-inositol

To determine whether the expression of the exogenous Na^+/myo-inositol cotransporter coding sequence indeed reflected transgene-expressed transport protein uptake activity, intralenticular myo-inositol content was determined in transgenic and nontransgenic age-matched littermates. Table 1 represents a compilation of intralenticular myo-inositol determinations taken from individual lenses from MLR21 mice taken from 8 to 11 weeks after birth. The intralenticular myo-inositol content of transgenic lenses was significantly elevated compared to nontransgenic lenses ($P < 0.001$), using an ANOVA and multiple group comparisons. Table 1 also shows a second compilation of intralenticular myo-inositol determinations taken from

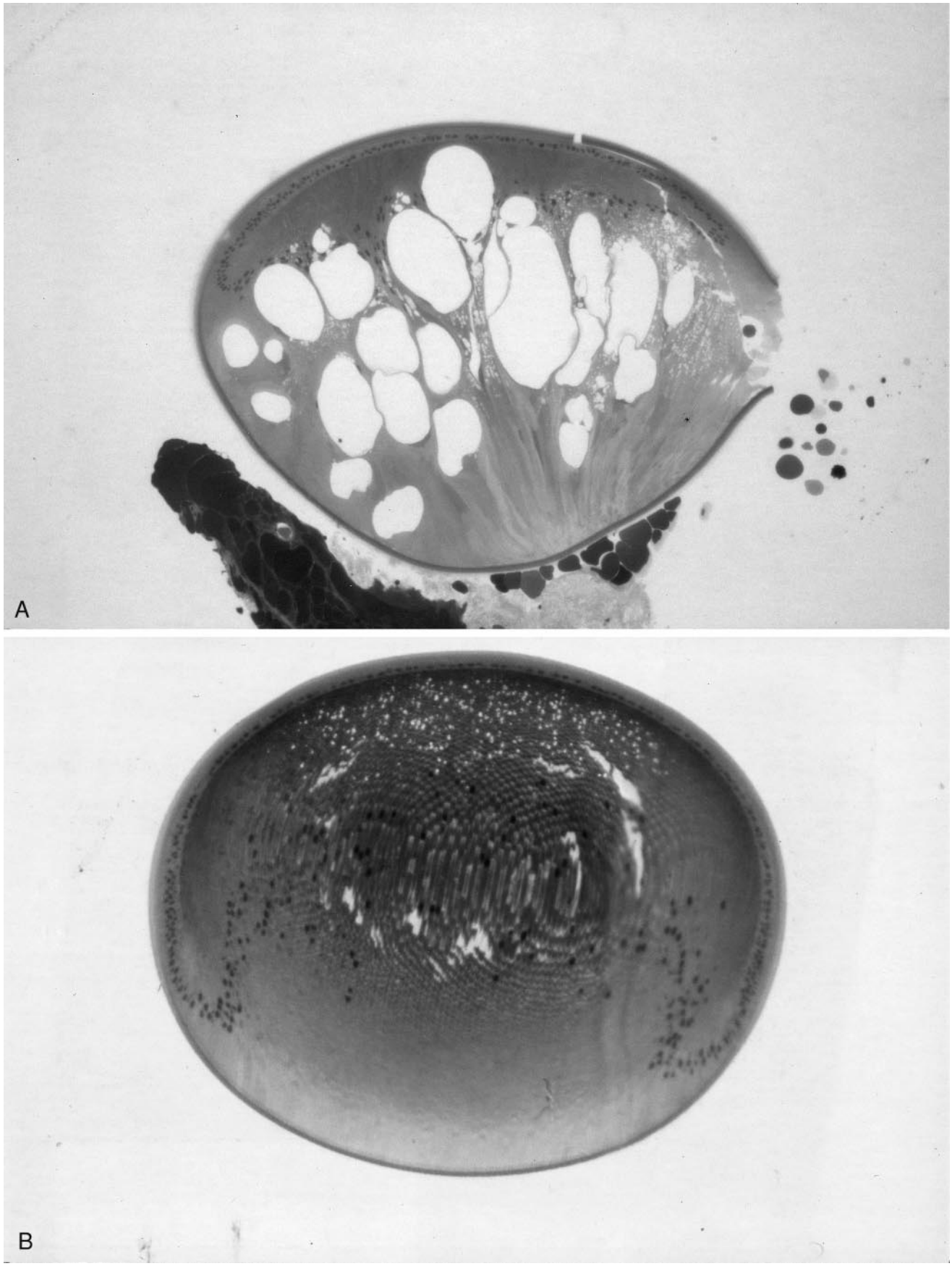

FIGURE 3. Transgenic mouse nuclear cataract. Thick-section light micrographs taken along the polar (visual) axis of a transgenic (**A**) and nontransgenic (**B**) 7-week-old mouse. Sections were stained with toluidine blue and hematoxylin.

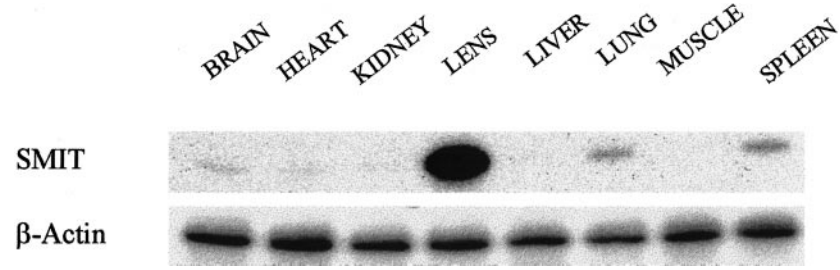

FIGURE 4. Bovine Na^+/myo-inositol cotransporter transgene expression of a variety of tissues taken from a transgene-positive MLR21 mouse. Total RNA was isolated from randomly sampled tissues, and a coupled RT–PCR was performed in the presence of α-^{32}P-dATP. The PCR products were separated on a denatured polyacrylamide gel. The bands were visualized by exposure to x-ray film. β-Actin mRNA expression was monitored to measure consistency of lane loading.

the lenses of the family MLR14. The intralenticular myo-inositol content of transgenic lenses was also significantly elevated compared to nontransgenic lenses of age-matched littermates ($P < 0.001$). However, it should be noted that the myo-inositol content of transgenic lenses from MLR14 was significantly below that of transgenic lenses from MLR21 ($P < 0.001$). The intralenticular myo-inositol content of nontransgenic lenses from the family MLR14 was comparable and not statistically different from the myo-inositol content of nontransgenic lenses from MLR21 ($P = 0.374$). Therefore, the hemizygous offspring from both of these transgenic lines show increased intralenticular myo-inositol accumulation, with the greatest increase in intralenticular myo-inositol correlating with the cataractous phenotype. Furthermore, the increased intralenticular myo-inositol content in the transgenic lenses from both families strongly suggests that functional Na^+/myo-inositol cotransporter protein expression was being directed by the transgenic construct.

Histologic Evaluation of Transgenic Lenses

Nuclear cataracts present in MLR21 transgenic mice on eyelid opening at 2 weeks of age indicated that lens pathology most likely occurred during or shortly after embryogenesis. Therefore, to evaluate developmental changes induced by expression of the CPV14/bSMIT transgene, ocular histology of E15.5 embryos from both transgenic families was analyzed (Fig. 7). The histologic structure of the lenses from MLR21 transgenic embryos (Figs. 7B, 7C) differed from those of MLR14 transgenic embryos (Figs. 7E, 7F) and nontransgenic embryos (Figs. 7H, 7I), both in the bow region and central zone of the lens, respectively. The MLR21 transgenic lenses were markedly swollen in the differentiating fiber cells of the bow region and subcapsular primary fibers of the central zone. The lens (Fig. 7A) appeared to have swollen cells extending from the subcapsular zone toward the posterior capsule. In addition, pyknotic nuclei could be seen within the fiber cells from the central zone of the MLR21 lenses (Fig. 7C). In contrast, the lenses from transgenic (Figs. 7D, 7F) and nontransgenic (Figs. 7G, 7I) littermates from family MLR14 exhibited normal histologic architecture.

DISCUSSION

Several independent transgenic founder mice were produced with the CPV14/bSMIT construct. Transgenic lines established from three of these founders spontaneously develop nuclear cataracts under normal feeding and housing conditions. Al-

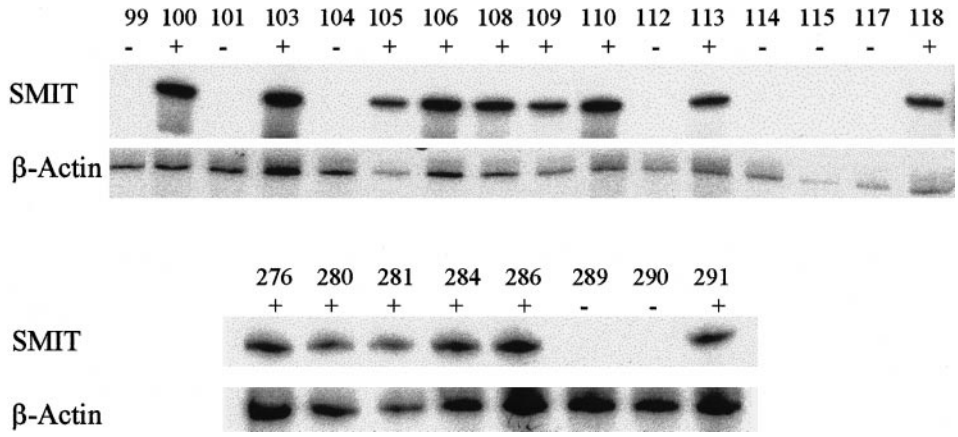

FIGURE 5. Bovine Na^+/myo-inositol cotransporter transgene and β-actin expression in transgenic and nontransgenic mouse lenses. Total RNA was isolated from individual lenses of age-matched littermates from the families MLR14 (*bottom panel*) and MLR21 (*top panel*). A coupled RT–PCR was performed in the presence of α-^{32}P-dATP. The PCR products were separated on a denaturing polyacrylamide gel. The bands were visualized by exposure to x-ray film.

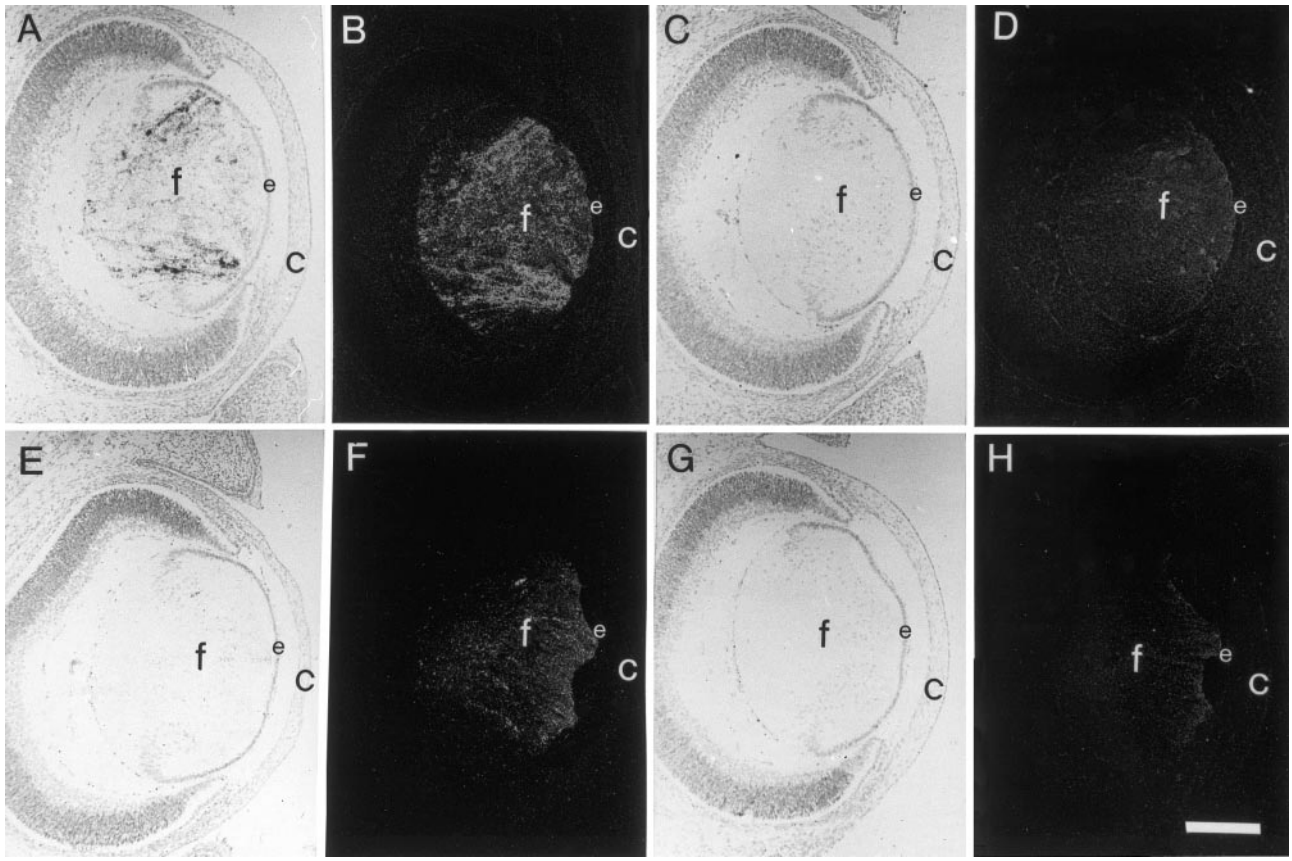

FIGURE 6. In situ hybridization of embryonic mouse eyes. Embryonic mouse eyes at E15.5 hybridized to transgene-specific antisense (**A**, **B**, **E**, **F**, **G**, **H**) or sense (**C**, **D**) riboprobes. Each tissue section is visualized with brightfield (**A**, **C**, **E**, **G**) and darkfield (**B**, **D**, **F**, **H**) photomicroscopy. Transgene-specific hybridization is indicated by exposed silver grains that appear *dark in brightfield* and *light in darkfield*. Eyes were examined from MLR21 transgenic (**A**, **B**, **C**, **D**), MLR14 transgenic (**E**, **F**), and nontransgenic (**G**, **H**) embryos. Strong transgene expression was detected in MLR21 lenses, whereas relatively weak transgene expression was evident in transgenic MLR14 lenses (compare **A** and **B** to **E** and **F**). No specific hybridization signals were detected with a sense riboprobe (**C**, **D**) or with an antisense riboprobe on nontransgenic lenses (**G**, **H**). Scale bar, (**H**) 20 μm.

though it is possible that a single transgenic line might develop cataracts as the result of a random insertional mutation, rather than from a specific consequence of transgene expression, three independently derived transgenic lines displaying a similar phenotype strongly argue against this possibility. Detailed analyses conducted on a cataractous (MLR21) and a noncataractous (MLR14) transgenic line demonstrated that transgenic transcripts were present in both lines. Furthermore, increased intralenticular myo-inositol accumulation in both of these lines is indicative of transgene-derived functional Na^+/myo-inositol cotransporter protein. In addition, transgenic lenses from the cataractous transgenic family MLR21 were shown by two different assays to express higher levels of transgene transcripts and also to accumulate higher myo-inositol levels than transgenic lenses from the noncataractous family MLR14.

TABLE 1. Lens Myo-inositol Content in Normal and Transgenic Mice

	Myo-inositol, nmol/mg lens wet wt
MLR14	
NTG	2.75 ± −0.86 (n=14)
TG	5.03 ± −0.97 (n=15)
MLR21	
NTG	3.30 ± −0.81 (n=13)
TG	8.67 ± −0.89 (n=12)

NTG, nontransgenic; TG, transgenic.

Results from these experiments support a role for osmotic stress in cataractogenesis. The degree of lens bSMIT gene expression and intralenticular myo-inositol content correlated positively with cataractous development, corroborating that accumulation of intracellular osmolytes is a major contributing factor for diabetic cataract. Using a customized lens promoter vector, which restricted transgene expression to the lens fibers, we demonstrated that the fibers of the lens are incapable of adequately compensating for the intrafiber osmotic stress incurred by the elevated expression of the exogenous Na^+/myo-inositol cotransporter gene. The resultant profound cellular swelling and consequent nuclear cataract development support the model that the lens fibers are innately susceptible to osmotic damage in an animal otherwise maintained under normal rearing conditions and diet.

Our experimental results should not be misconstrued as an affirmation that myo-inositol accumulation is the cause of diabetic cataract. Rather, it is well documented that increased

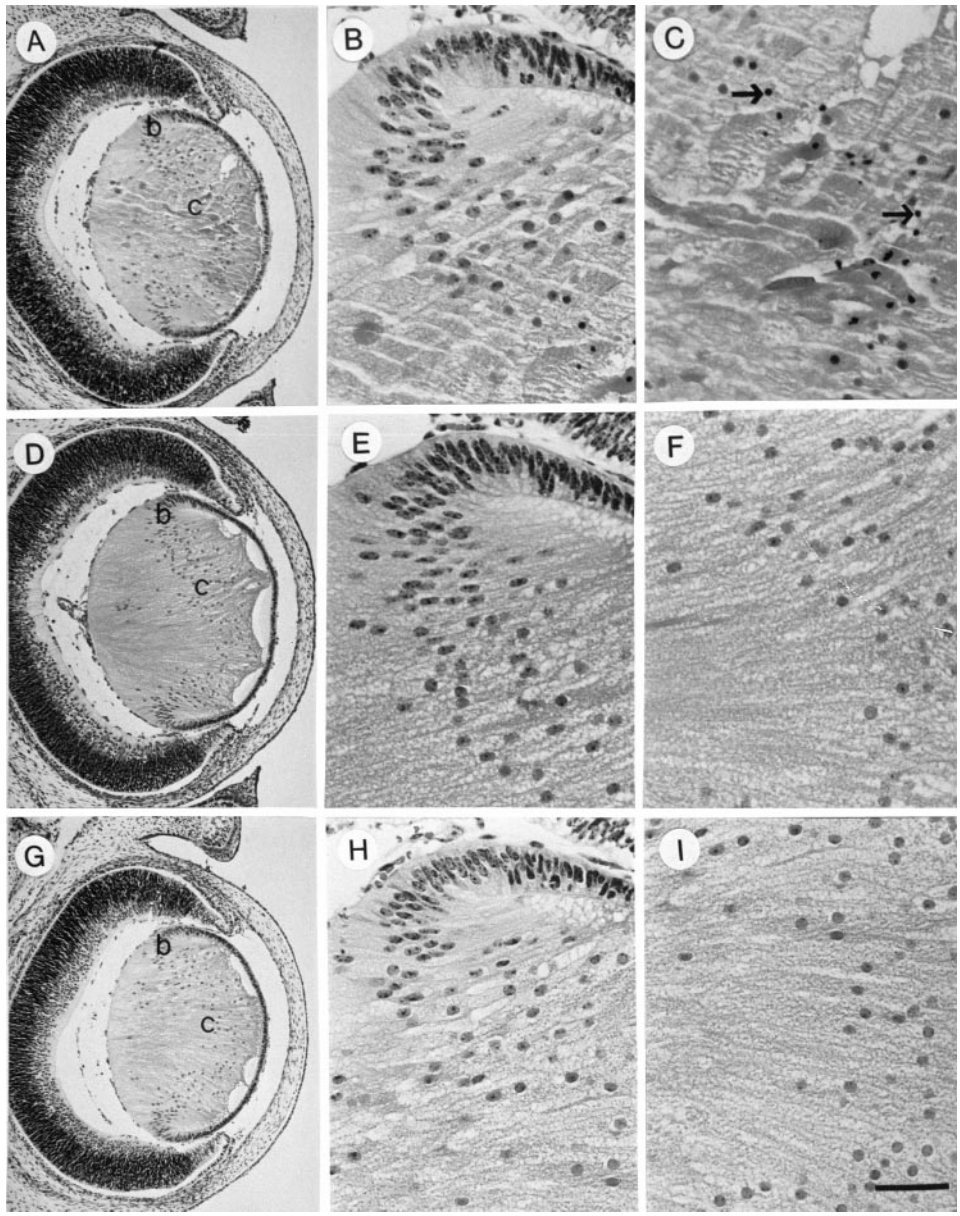

FIGURE 7. Hematoxylin and eosin (H and E)–stained tissue sections of embryonic mouse eyes. H and E–stained tissue sections of eyes from E15.5 MLR21 transgenic (**A**, **B**, **C**), MLR14 transgenic (**D**, **E**, **F**), and nontransgenic (**G**, **H**, **I**) embryos. Each eye is represented by one low-power magnification (**A**, **D**, **G**) and two high-power magnification views representing the bow region (**B**, **E**, **H**) and the central primary fibers (**C**, **F**, **I**). The transgenic eye from MLR21 displays no obvious abnormalities in the lens epithelium, but the primary lens fiber cells appear swollen (**B**, **C**) when compared to the primary fiber cells of the MLR14 transgenic (**E**, **F**) and nontransgenic (**H**, **I**) eyes. In addition, the nuclei of the primary fiber cells from MLR21 appear condensed and pyknotic (*arrows* in **C**), whereas the corresponding nuclei from MLR14 (**F**) and nontransgenic lenses (**I**) are larger and less densely stained. No obvious consistent differences were observed between MLR14 transgenic and nontransgenic lenses at E15.5. The separation of lens epithelium from fiber mass and the vacuolization present between the lens epithelium and the lens fiber cells were present in all sections examined and therefore represent fixation, processing artifact, or both. Scale bar, (**A**, **D**, and **G**) 20 μm; (**B**, **C**, **E**, **F**, **H**, and **I**) 5 μm.

aldose reductase activity and reduced tissue myo-inositol are the causative factors that contribute to early-onset diabetic complications in the lens and other tissues.[17–21] Hyperglycemia promotes polyol accumulation, which causes a reduction in intracellular myo-inositol content.[22–24] Decreased tissue-free myo-inositol is a common identifiable complication associated with hyperglycemia in nonocular[25,26] and ocular[27] tissue alike. A decline in intralenticular myo-inositol has been demonstrated with rat lenses maintained in organ culture and exposed to extralenticular galactose; the depletion of lenticular myo-inositol has been shown to be prevented by the coadministration of an aldose reductase inhibitor.[19] Studies from this laboratory have previously determined that exposure of cultured bovine lens epithelial cells to high ambient galactose[17,28] or glucose[3,4] elicited the reversible impairment of myo-inositol transport, thereby providing a plausible mechanism whereby the rapid loss of intracellular myo-inositol associated with hyperglycemia could be explained. Severe intracellular polyol accumulation also activates the chloride channel–associated myo-inositol efflux pathway (Reeves RE and Cammarata PR, unpublished observations), further prompting the loss of myo-inositol from cell to surrounding environment.

Lee et al.[29] have previously shown that transgenic mice over-expressing aldose reductase in the lens became susceptible to the development of diabetic and galactose cataracts. Unlike the transgenic animals in this study, their mice did not develop cataracts under normal rearing conditions. Rather, they reported a slow progression of cataract morphologically separable into three stages: peripheral vacuolization, vacuoles covering the entire lens and fusing together, and complete lens opacity. However, none of these three stages was observed unless the mice were fed a 50% galactose diet. Transgenic mice made diabetic by streptozotocin injection developed cataracts even less readily than did galactosemic mice. Clearly, cataract development in that animal model was rate limited either by substrate availability for the aldose reductase reaction or by the relatively low expression of the transgene. However, the pace of cataract formation notwithstanding, they correctly con-

cluded that cataract development was proportional to the level of aldose reductase activity and sorbitol accumulation. Our data, likewise, authenticate a role for osmolyte accumulation in the advancement of diabetic cataract, in that a positive correlation between Na^+/myo-inositol cotransporter gene expression (i.e., transporter activity) and myo-inositol over-accumulation could be linked to progression of cataract development. The development of nuclear cataract in the CPV14/bSMIT TG mice was unexpectedly swift and severe considering that a myo-inositol–supplemented diet was not provided for the birth mother. The generation of nuclear cataract was evident as early as E15.5 (the earliest time examined in this study) in the differentiating secondary fibers, an observation consistent with the midgestation expression of the endogenous murine αA-crystallin gene.[30] Strong transgene expression in the embryonic lens, in a region of the lens already compromised in its ability to cope with the imposing intrafiber osmolyte over-accumulation, apparently influences fiber swelling at an early stage of development, producing a profound nuclear cataract in neonates.

The animal model we have described may have unique applications. The range of bSMIT transgene expression and corresponding lenticular phenotype should make these animals invaluable models to study the influence of diet, drugs, and other factors on the osmotic homeostasis of the lens.

To our knowledge, these mice provide the first demonstration of experimental cataractogenesis attributable to overexpression of the Na^+/myo-inositol cotransporter gene in the lens of transgenic mice. Indeed, our observation may have interesting medical relevance in that those people afflicted with Down's Syndrome (DS) exhibit trisomy 21, and of them many develop cataract. The gene for the Na^+/myo-inositol cotransporter maps to chromosome 21[31]; therefore, there are three copies of this gene in DS individuals compared with the normal two copies in the disease-free state. Thus, individuals with DS over-accumulate and retain abnormally high levels of myo-inositol.[32] The DS-associated cataract has been reported to be quite variable and unique.[33]

Acknowledgments

The authors thank Janet Weslow–Schmidt for the production of the transgenic mice and William Olson for his expert technical assistance. They also thank Jerry W. Simecka for performing the statistical ANOVA and group comparisons of the subsets of intralenticular myo-inositol determinations.

References

1. Garcia–Perez A, Burg MB. Role of organic osmolytes in adaptation of renal cells to high osmolarity. *J Membrane Biol.* 1991; 119:1–13.
2. Carper D, Kaneko M, Stark H., Hohman T. Increase in aldose reductase mRNA in dog lens epithelial cells under hypertonic conditions. *Exp Eye Res.* 1990;50:743–749.
3. Cammarata PR, Chen H–Q, Yang J, Yorio T. Modulation of myo[^{3}H]inositol uptake by glucose and sorbitol in cultured bovine lens epithelial cells, I: restoration of myo-inositol uptake by aldose reductase inhibition. *Invest Ophthalmol Vis Sci.* 1992;33:3561–3571.
4. Cammarata PR, Chen H–Q, Yang J, Yorio T. Modulation of myo-[^{3}H]inositol uptake by glucose and sorbitol in cultured bovine lens epithelial cells, II: characterization of high- and low-affinity myo-inositol transport sites. *Invest Ophthalmol Vis Sci.* 1992;33:3572–3580.
5. Yokoyama T, Lin L–R, Bhargavan C, Reddy V. Hypertonic stress increases NaK ATPase, taurine, and myo-inositol in human lens and retinal pigment epithelial cultures. *Invest Ophthalmol Vis Sci.* 1993;34:2512–2517.
6. Cammarata PR, Chen H–Q. Osmoregulatory alterations in myo-inositol uptake by bovine lens epithelial cells, I: a hypertonicity-induced protein enhances myo-inositol transport. *Invest Ophthalmol Vis Sci.* 1994;35:1223–1235.
7. Zhou C, Chen H–Q, Reeves R, Agarwal N, Cammarata PR. Osmoregulatory alterations in myo-inositol uptake by bovine lens epithelial cells, Part 4: induction pattern of Na^+-myo-inositol cotransporter mRNA under hypertonic conditions denoting an early-onset, interactive, protective mechanism against water stress. *Invest Ophthalmol Vis Sci.* 1994;35:4118–4125.
8. Reeves R, Cammarata PR. Osmoregulatory alterations in myo-inositol uptake by bovine lens epithelial cells, Part 5: mechanism of the myo-inositol efflux pathway. *Invest Ophthalmol Vis Sci.* 1996; 37:619–629.
9. Cammarata PR, Xu G–T, Huang L, Zhou C, Martin, M. Inducible expression of Na^+/myo-inositol cotransporter mRNA in anterior epithelium of bovine lens: affiliation with hypertonicity and cell proliferation. *Exp Eye Res.* 1997;64:745–757.
10. Zhou C, Agarwal N, Cammarata PR. Osmoregulatory alterations in myo-inositol uptake by bovine lens epithelial cells, Part 2: cloning of a 626 bp cDNA portion of a Na^+/myo-inositol cotransporter, an osmotic shock protein. *Invest Ophthalmol Vis Sci.* 1994;35:1236–1242.
11. Zhou C, Cammarata PR. Cloning the bovine Na^+/myo-inositol cotransporter gene and characterization of an osmotic responsive promoter. *Exp Eye Res.* 1997;35:349–363.
12. Robinson ML, Overbeek PA, Verran DJ, et al. Extracellular FGF-1 acts as a lens differentiation factor in transgenic mice. *Development.* 1995;121:505–514.
13. Cvekl A, Sax CM, Bresnick EH, Piatigorsky J. A complex array of positive and negative elements regulates the chicken alpha A-crystallin gene: involvement of Pax-6, USF, CREB and/or CREM, and AP-1 proteins. *Mol Cell Biol.* 1994;14:7363–7376.
14. Robinson ML, Reneker LW, Majumder K, et al. Engineering the A-crystallin promoter to express in the lens epithelium of transgenic mice[ARVO Abstract]. *Invest Ophthalmol Vis Sci.* 1997; 38(4):**S**579, Abstract nr 2694.
15. Gorman CM, Moffat LM, Howard BH. Recombinant genomes which express chloramphenicol acetyltransferase in mammalian cells. *Mol Cell Biol.* 1982;2:1044–1051.
16. Robinson ML, Ohtaka–Maruyama C, Chan CC, et al. Disregulation of ocular morphogenesis by lens-specific expression of FGF-3/int-2 in transgenic mice. *Dev Biol.* 1998;198(1):13–31.
17. Cammarata PR, Tse D, Yorio T. Sorbinil prevents the hypergalactosemic-induced reduction in [^{3}H]-myo-inositol uptake and decreased [^{3}H]-myo-inositol incorporation into the phosphoinositide cycle in bovine lens epithelial cells in vitro. *Curr Eye Res.* 1990; 9:561–568.
18. Winegrad AL. Banting Lecture 1986: does a common mechanism induce the complications of diabetes? Diabetes 1987:36: 396–406.
19. Kawaba T, Cheng H–M, Kinoshita JH. The accumulation of myoinositol and rubidium ions in galactose-exposed rat lens. *Invest Ophthalmol Vis Sci.* 1986;27:1522–1526.
20. MacGregor LC, Matschinsky FM. Treatment with aldose reductase inhibitor or with myo-inositol arrest deterioration of the electroretinogram of diabetic rats. *J Clin Invest.* 1985;76:887–889.
21. Finegold D, Lattimer SA, Nolle S, Bernstein M, Greene DA. Polyol pathway and myo-inositol metabolism: a suggested relationship in the pathogenesis of diabetic neuropathy. *Diabetes.* 1983;32:988–992.
22. Okuda Y, Bannai C, Nagahama M, Isaka M, Yamashita K. Restoration of myo-inositol uptake by aldose reductase inhibitor in human skin fibroblasts cultured in high-glucose medium. *Horm Metab Res.* 1991;23:42–43.

23. Yorek MA, Dunlap JA, Ginsberg BH. Effect of sorbinil on myo-inositol metabolism in cultured neuroblastoma cells exposed to increased glucose levels. *J Neurochem.* 1988;51:331–338.
24. Greene DA. A sodium-pump defect in diabetic peripheral nerve corrected by sorbinil administration: relationship to myo-inositol metabolism and nerve conduction slowing. *Metabolism.* 1986;35: 60–65.
25. Yue DK, Hanwell MA, Satchell PM, Handelsman DJ, Turtle JR. The effects of aldose reductase inhibition on nerve sorbitol and myo-inositol concentrations in diabetic and galactosemic rats. *Metabolism.* 1984;33:1119–1122.
26. Llewelyn JG, Simpson CMF, Thomas PK, King RHM, Hawthorne JN. Changes in sorbitol, myo-inositol and lipid inositol in dorsal root and sympathetic ganglia from streptozotocin-diabetic rats. *Diabetetologia.* 1986;29:876–881.
27. Li W, Chan LS, Khatami M, Rockey JH. Non-competitive inhibition of myo- inositol transport in cultured bovine retinal capillary pericytes by glucose and reversal by sorbinil. *Biochim Biophys Acta.* 1986;857:198–208.
28. Cammarata PR, Tse D, Yorio T. Uncoupling of attenuated myo-[^{3}H]inositol uptake and dysfunction in Na^+K^+-ATPase pumping activity in hypergalactosemic cultured bovine lens epithelial cells. *Diabetes.* 1991;40:731–737.
29. Lee AYW, Chung SK, Chung SSM. Demonstration that polyol accumulation is responsible for diabetic cataract by the use of transgenic mice expressing the aldose reductase gene in the lens. *Proc Natl Acad Sci USA.* 1995;92:2780–2784.
30. Treton JA, Jacquemin E, Courtois Y, Jeanny J. Differential localization by in situ hybridization of specific crystallin transcripts during mouse lens development. *Differentiation.* 1991;47:143–147.
31. Berry GT, Mallee JJ, Blouin J–L, Antonarakis SE. The 21q22.1 STS marker, VN02 (EST00541 cDNA), is part of the 3′ sequence of the human Na^+/myo-inositol cotransporter (SLC5A3) gene. *Cytogenet Cell Genet.* 1996;73:77–78.
32. Shetty HV, Schapiro MB, Holloway HW, Rapoport SI. Polyol profiles in Down Syndrome: myo-inositol, specifically, is elevated in the cerebrospinal fluid. *J Clin Invest.* 1995;95:542–546.
33. Janjani A, Duglas–Tabor Y, Garland DL. Lens in Down's Syndrome. *Invest Ophthalmol Vis Sci.* 1997;38(4):**S**585, Abstract nr 2726.